RESEARCH ARTICLE

Optimization of Telmisartan Loaded Locust Bean Gum and Thiolated Chitosan Hydrogel Using Central Composite Design

Mohanraj V, Komala M*

Department of Pharmaceutics, Vels Institute of Science, Technology & Advanced Studies, Chennai, India.

Received: 18th Aug, 2024; Revised: 9th Oct, 2024; Accepted: 12nd Nov, 2024; Available Online: 25th Dec, 2024

ABSTRACT

This article describes the formulation of a mucoadhesive thiolated chitosan (TC) and Locust Bean Gum (LBG) hydrogel for the application of site-targeted delivery of telmisartan. The hydrogel was formulated using the tripolyphosphate (TPP) ionotropic gelation cross-linking procedure. The optimized IPN hydrogel was considered by FTIR, UV-visible and SEM. And *in vitro* drug release abilities and mucoadhesion properties were also evaluated. The effect of polymer blend ratio on swelling capacity was investigated. The improved formulation demonstrated long-lasting drug release (up to 12 hours) and excellent mucoadhesiveness. A non-fickian technique was used to monitor the drug release from the hydrogel. The study's findings suggest that LBG:TC hydrogel could be a good vehicle for targeted medication delivery.

Keywords: Thiolated chitosan; locust gum; IPN hydrogel; telmisartan; Ionic gelation

How to cite this article: Mohanraj V, Komala M. Optimization of Telmisartan Loaded Locust Bean Gum and Thiolated Chitosan Hydrogel Using Central Composite Design. International Journal of Drug Delivery Technology. 2024;14(4):2081-90. doi: 10.25258/ijddt.14.4.20

Source of support: Nil

Conflict of interest: None

INTRODUCTION

Locally targeted drug delivery and controlled drug delivery are considered superior drug therapy in terms of their higher efficacy in treating death with minimal drug dose and low toxicity. These attractive features will increase the patient's affordability of a particular therapy and complaint. As compared to other methods of drug administration, oral route is utmost appealing to researchers due to its easiness of administration and fact that it allows for the formulation of varied doses of the drug. The ideal regulated drug delivery system would keep target medication's plasma concentration constant for a long period.[1] Oral drug delivery system development for a particular medicine typically hinges on optimising the dosage form to be created in conjunction with the gastrointestinal physiology of the target site of delivery. Gastric residence time is one of the factors to be considered before designing oral sustained drug administration, the successful achievement of which is essential. Due to the rapid passage of the drug through the gastrointestinal tract, it may prevent the drug from being fully released from the designed dose at the site that was targeted for release, possibly reducing the effectiveness of the administered dose, as most drugs are absorbed in stomach/ upper small intestine.[2] To circumvent these issues, scientists have developed gastroretention drug delivery systems. These systems can stay in stomach for several hours according to the program, which greatly extends the medication's residence period there. Oral gastroretention drug delivery systems can prolong a medication's GRT by tailored dosing, which in turn improves the dose form's predictability and bioavailability. Because it reduces intersubject variability and so-called "peak and valley" effect, this is especially true for molecules with a narrow absorption window. Also, medications that have trouble dissolving in acidic environments will have their solubility enhanced if their overall transit time through the GI tract is prolonged.[3] An antihypertensive medication belonging to the BCS class II with poor solubility, telmisartan is measured as 4'-{[4-methyl-6-(1-methyl-2-benzimidazolyl)-2-propyl-1-benzimidazolyl] methyl}-2-biphenylcarboxylic acid.[4,5] Due in large part to its low bioavailability following oral administration, this drug's low solubility in biological fluids is one of its primary drawbacks. Only 0.078 mg of telmisartan is soluble in each milliliter of water, which is considered very low to meet bioavailability. Due to the low solubility, the absolute bioavailability of ores was only 42-58%. This leads to poor dissolution and thus differences in bioavailability have been observed at its conventional doses.[6] Telmisartan has been found to be more soluble and bioavailable in a variety of formulations, including immediate-release tablets[7], nanoparticles,[8,9] nanoemulsion drug delivery systems,[10] amorphous powders,[11] solid dispersions,[12] or alkalisers.[13] Because of anionic drug and significant positive charge of polymer, electrostatic interactions between TEL and CS led to formation of telmisartan-chitosan solid dispersions.[14] In addition to the methods already mentioned, one effective method of increasing the medicine's bioavailability is the gastro retentive drug delivery system, which allows the drug to spend more time in GIT. One gastro retentive formulation that has garnered a lot of interest from drug delivery scientists in the last several decades is hydrogels. These polymeric networks are three-dimensional and hydrophilic, meaning they can absorb a lot of water or bodily fluids. Insoluble homopolymers or copolymers with chemical or physical crosslinks (such as tie-points or junctions) make up

*Author for Correspondence: komala.sps@velsuniv.ac.in

hydrogel networks. These cross links provides them a network structure and physical integrity. Because their thermal properties are compatible with water, they can swell in specific mediums.[15] Particularly in the fields of medicine and pharmaceuticals, these hydrogels have numerous uses. When compared to other types of synthetic biomaterials, hydrogels are the most lifelike. The reason behind this is that they resemble real tissue in their softness and high water content. Furthermore, materials' biocompatibility is enhanced by their high water content.[16] Hydrogels have a extensive choice of potential applications, including medication delivery devices, contact lenses, biosensor membranes, artificial heart linings, and materials for artificial skin. Due to their unique properties, they have found application in various ways of drug administration.[17-20] Based on their requirements, the hydrogel can be formulated either using only natural polymers or synthetic biopolymers, or using a single biopolymer or a combination of two or more biopolymers[21]. In general, hydrogels formulated using natural polymers are more economical and biocompatible than their synthetic counterparts.[22]

Chitosan is an interesting polymer with greater properties that can be formulated as a hydrogel, as a simple hydrogel, and as hydrogels with other natural and synthetic polymers. But while it is formulated as a hydrogel alone, it will face the problem of high gastric solubility, which will lead to rapid release, which is not suitable for enhancing biocompatibility for poorly soluble drugs.[23] Furthermore, its cationic amine (hydrophilic) functional group will not allow effective loading of the hydrophobic drug. To overcome this problem, many surface functionalization of chitosan have been proposed in literature, such as carboxylation, alkylation, quaternization, thiolation, and so on.[24,25] Among the surface-functionalized chitosan derivatives, thiolated chitosans are of great interest in terms of their superior mucoadhesive properties compared to the native polymer.[26,27] Due to the high porosity, single thiolated ones will not be applicable for sustained drug delivery for a lengthier era of time, so polymer combinations have been proposed to develop interpenetrating networks with other polymers using physical and chemical cross-linking. Locust bean gum is one of the polymers of choice for creating an interpenetrating gel network for sustained-release gastroretentive hydrogels. In this regard, an IPN hydrogel of oxidized dextran cross-linked thiolated chitosan and St. John's wort has been reported for its hemostatic use.[28] However, no one has yet detailed how to use them as a

Table 1. Central Composite Design experimental design

Independent factors	Unit	Levels		
		Low	Medium	High
X_1 = Amount of LBG	%	1	1.25	1.5
X_2 = Amount of TC	%	0.5	1	1.5
X_3 = Tripolyphosphate (TPP)	%	5	6.25	7.5
Responses (dependent factors)				
Y1 = Size	Micron			
Y2 = Mucoadhesive properties	%			
Y3 = Percentage of drug release	%			

Table 2. Optimization of LBG: TC IPN hydrogel using CCD Design

Std	Run	Factor 1 A:TC	Factor 2 B:LBG	Factor 3 C:TPP	Response 1 Mucoadhesive	Response 2 Particle Size	Response 3 Drug Release
		%	%	%	%	micron	%
17	1	1.25	1	6.25	62	220	96.24
18	2	1.25	1	6.25	62	220	96.24
5	3	1	0.5	7.5	46	256	89.9284
15	4	1.25	1	6.25	62	220	96.24
14	5	1.25	1	8.35224	24	215	54.9658
1	6	1	0.5	5	63	218	82.8264
2	7	1.5	0.5	5	32	219	69.1855
3	8	1	1.5	5	43	159	93.3002
19	9	1.25	1	6.25	62	220	96.24
20	10	1.25	1	6.25	62	220	96.24
13	11	1.25	1	4.14776	54	204	82.3293
10	12	1.67045	1	6.25	75	216	44.4065
11	13	1.25	0.159104	6.25	39	200	56.432
4	14	1.5	1.5	5	75	173	98.24
7	15	1	1.5	7.5	41	218	33.45
16	16	1.25	1	6.25	62	220	96.24
12	17	1.25	1.8409	6.25	54	153	99.86
6	18	1.5	0.5	7.5	51	207	31.6162
9	19	0.829552	1	6.25	42	209	87.654
8	20	1.5	1.5	7.5	62	147	38.37

medication delivery mechanism for pharmacological agents that are not particularly soluble. Our paper details an intravenous pulmonary formulation (IPN) of thiolated chitosan and locus gum hydrogel for the long-term administration of the poorly soluble hypertension medicine telmisartan. The formulation was evaluated for its mucoadhesiveness, swelling index, SEM morphology and drug release properties.

Materials and methods

Telmisartan was gifted from The Madras Pharmaceuticals, Chennai. Chitosan and locust bean gum was purchased from spectrum chemicals. All other chemical were purchased from Merck. Double distilled water was used and analytical grade solvents were used in this study.

Preparation of Thiolated Chitosan Polymer

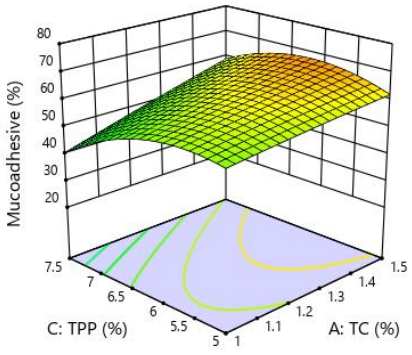

Figure 1: (a) Effect of TC and TPP concentration on Mucoadhesive properties

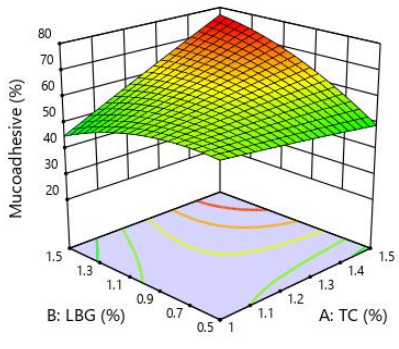

Figure 1: (b) Effect of LBG and TC concentration on Mucoadhesive properties

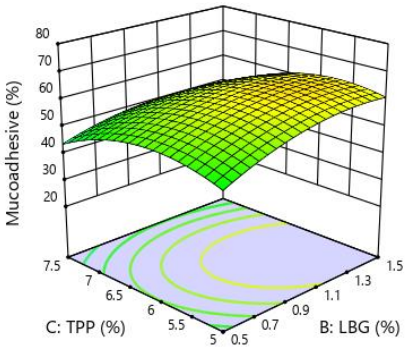

Figure 1: (c) Effect of LBG and TPP concentration on Mucoadhesive properties

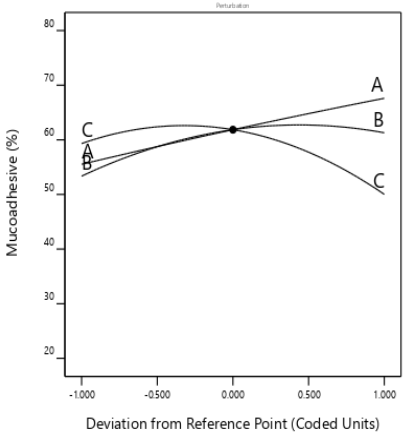

Figure 1 (d): Effect of LBG, TC and TPP concentration on Mucoadhesive properties

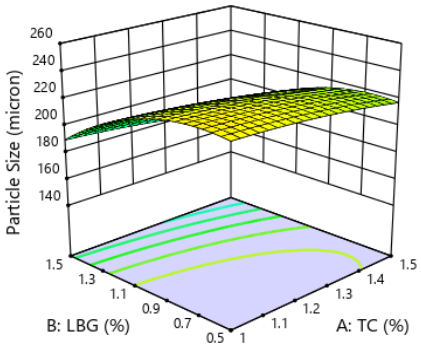

Figure 2: (a) Effect of LBG and TC concentration on size of hydrogel particles (µm)

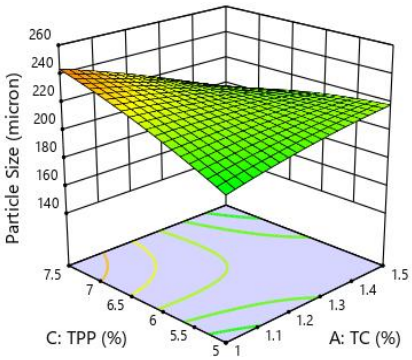

Figure 2: (b) Effect of TC and TPP concentration on size of hydrogel particles (µm)

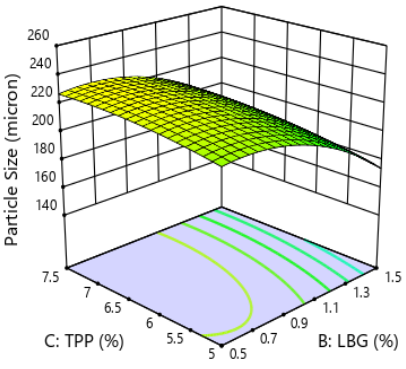

Figure 2: (c) Effect of LBG and TPP concentration on size of hydrogel particles (µm)

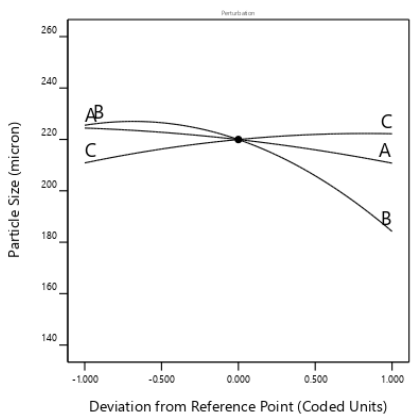

Figure 2: (d) Effect of LBG, TC and TPP concentration on size of hydrogel particles (µm)

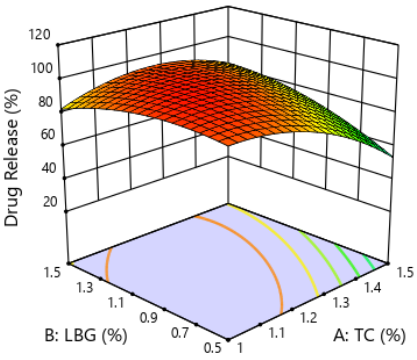

Figure 3: (a) Effect of LBG and TC concentration on Drug Release

Chitosan-cysteine conjugates were synthesized using EDAC click chemistry. In order to accomplish this, a solution was prepared by dissolving 5 grammes of chitosan in a 1% acetic acid solution, adding 5 grammes of cysteine to the mixture, and then adding 50 mM EDAC. By adding 1N NaOH, the pH was brought down to 5. The ingredients were vigorously mixed for three hours. To remove EDAC and free cysteine, the solution was dialysed in a light-protected dialysis tube ((Cellu/Sep Membrane Dialysis MWCO = 5000)). After being dried at 40 ℃ for 12 hours, filtrate solution was carefully sealed and kept in a container until it was needed. Following dialysis, the yield of thiolated chitosan was around 90%.[29]

Formulation of LBG: TC hydrogels

Experimental design (DOE)

An ideal LBG:TC IPN hydrogel for telmisartan mucoadhesive distribution was designed and developed using response surface approach. Three variables—the

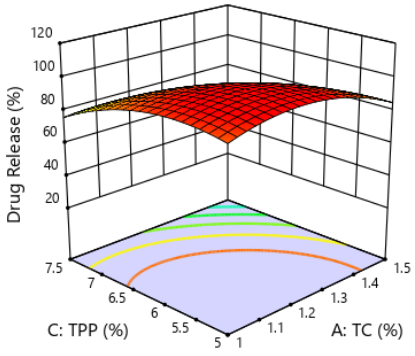

Figure 3: (b) Effect of TC and TPP concentration on Drug Release

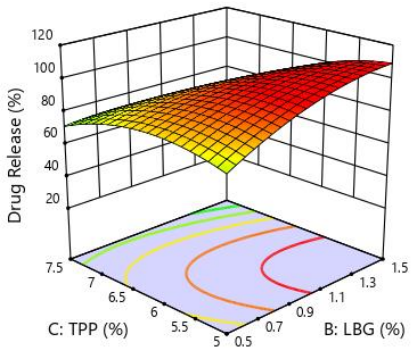

Figure 3: (c) Effect of LBG and TPP concentration on Drug Release

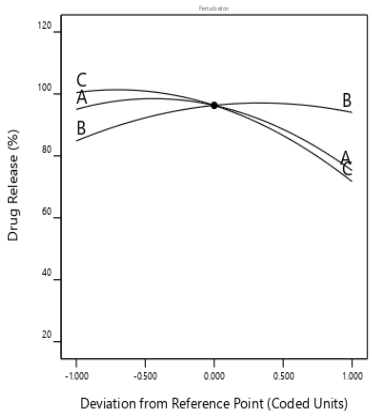

Figure 3: (d) Effect of LBG, TC and TPP concentration on Drug Release

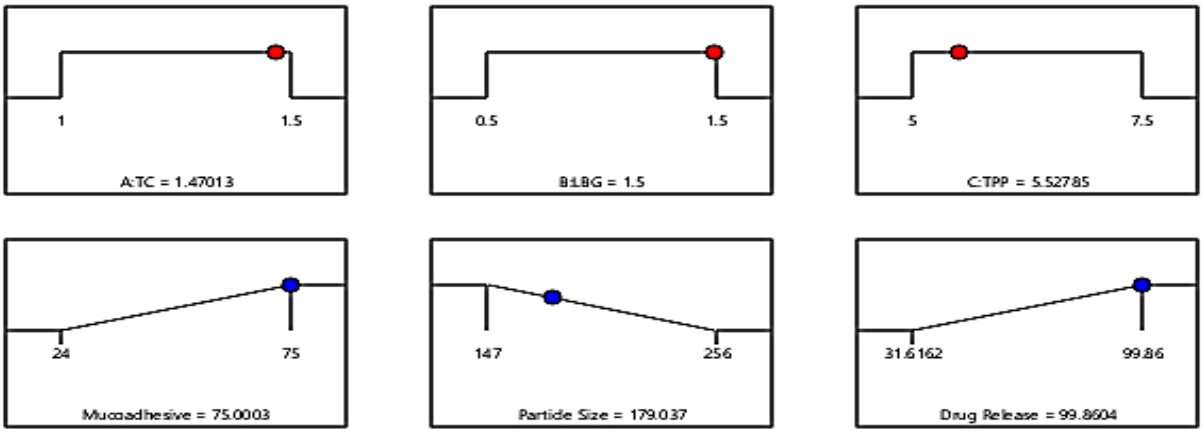

Figure 4: Optimum formulation derived by CCD (Desirability =0.917; Solution 1 out of 34)

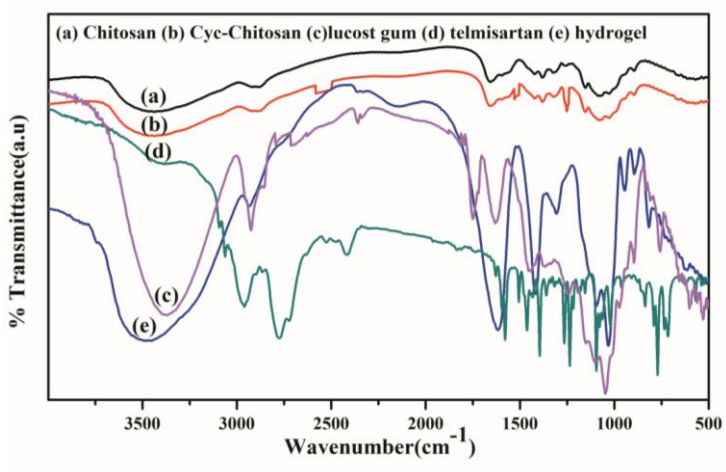

Figure 5: FTIR spectrum of (a) chitosan, (b) Thio-chitosan, (c) Locust bean gum, (d) telmisartan (e) LBG:TC hydrogel

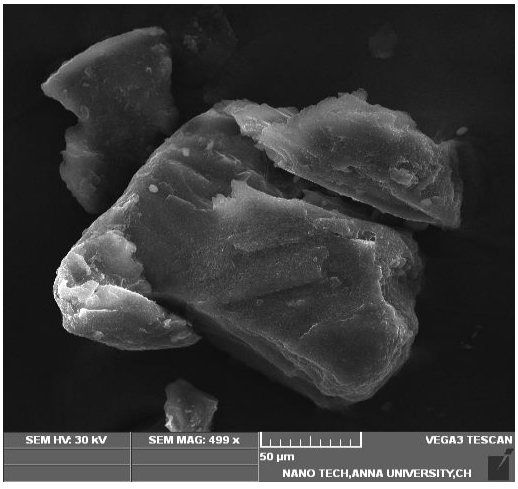

Figure 6: SEM images of LBG: TC hydrogel particles

amounts of carob gum, thiolated chitosan, and TPP—are used in the computational design strategy of the central composite design carried out using Design Expert Software (Table 1). In order to find the best formulation, researchers looked at how several independent factors affected responsiveness, mucoadhesive efficiency, particle size, and drug release.

Optimized procedure for hydrogel drug formulation

A solution of 1% aqueous acetic acid was prepared by dissolving a precisely measured amount of thiolated chitosan. A 25 mL solution of distilled water containing locust bean gum (LG) was prepared at 40 ℃. Two hours of stirring at 250 rpm was used to thoroughly combine the two polymer solutions that had been created. The solution's pH was about 4.2 before adding small volumes of 2 M NaOH solution, which brought the value up to 5.8. The next step was to make an aqueous solution of tripolyphosphate (TPP) with ultrapure water at a concentration of 0.5 mg/mL. After that, 5–7.5% of the solution was put in a refrigerator and cooled down to 0–2°C for four hours. For 10 minutes at 60°C with continuous stirring, polymer solution was heated in a water bath. After transferring solution to an ice bath, TPP solution was added immediately and agitated for 10 minutes. After removing the hydrogel from ice bath, it was allowed to dry at ambient temperature for an additional step. Preparation of LBG:TC TEL hydrogel, the above procedure was followed with the addition of telmisartan.

Characterization

To evaluate the possible interaction among drug and polymers used in formulations, FT-IR spectroscopy on drug, free polymer and hydrogel formulations was performed separately using an FTIR spectrophotometer (Jasco FTIR-4100, Japan). The research employed the KBr-pressed pallet technique. The Fourier transform infrared spectra were scanned 40 times over the 4000-400 cm-1 wavenumber range. SEM, Jeol Jsm-840, Japan was also used to examine surface morphology of hydrogel that was made. Using double-sided adhesive carbon tape, a small quantity of the hydrogel sample was splattered across the aluminium SEM attachment. Before the sample was analysed using a scanning

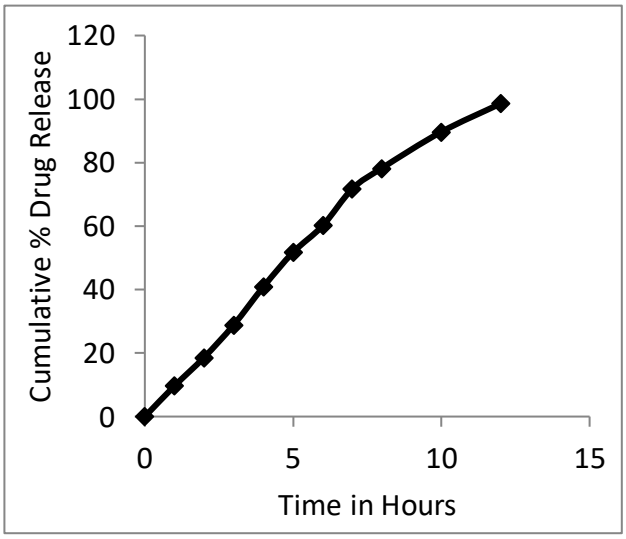

Figure 7: *In vitro* drug release of TEL from LBG:TC hydrogels

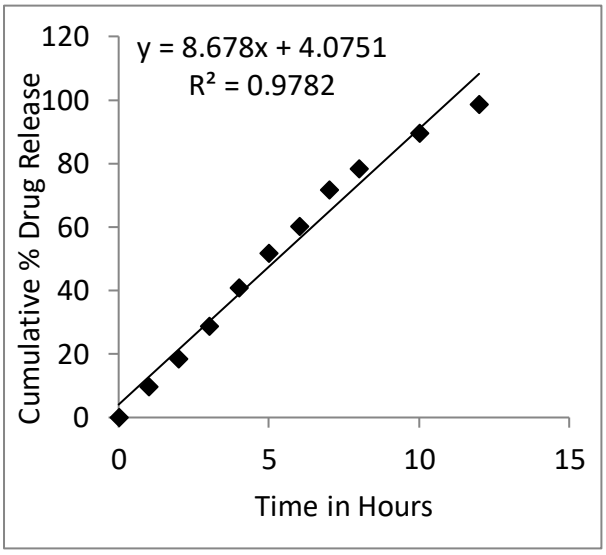

Figure 8: *In vitro* Zero order drug release kinetics

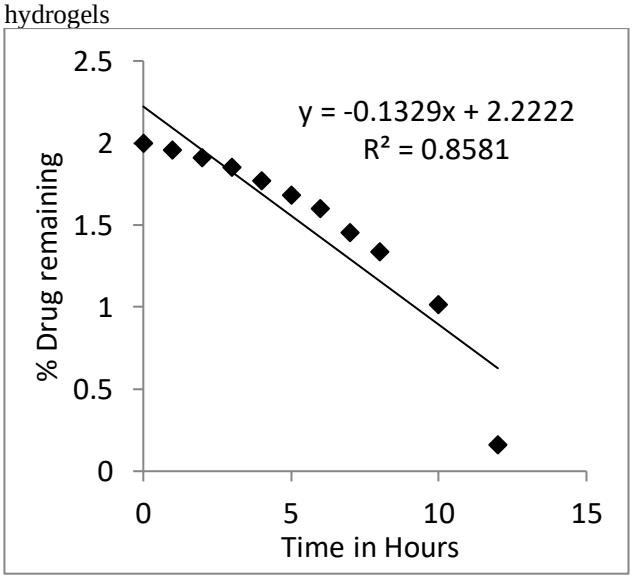

Figure 9: *In vitro* First order drug release kinetics

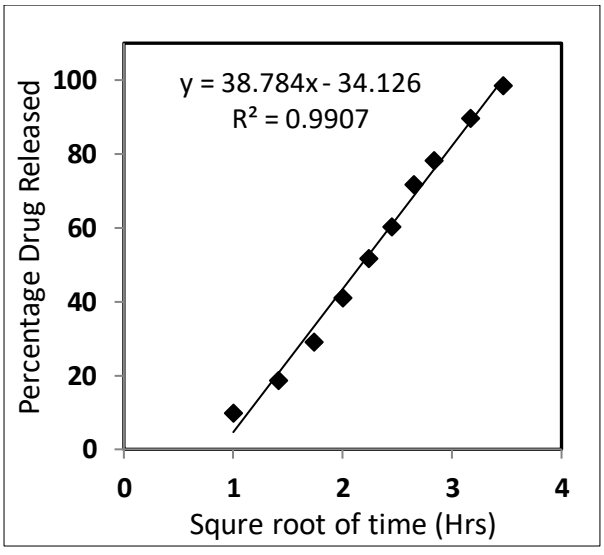

Figure 10: *In vitro* Higuchi drug release kinetics

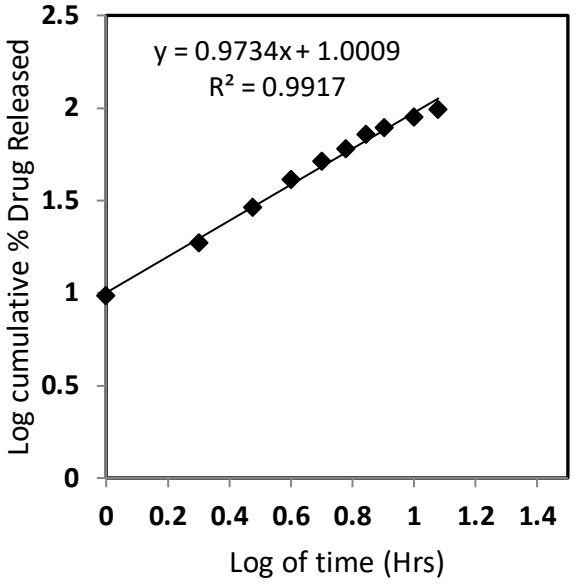

Figure 11: *In vitro* Korsmeyer-Peppas drug release kinetics

electron microscope (SEM), it was sputtered with gold plasma.

Determination of entrapment efficiency

A roundabout way was employed to ascertain the quantity of medication trapped within the hydrogels. The washings are collected after the gel preparation and passed through a 0.45 µm millipore filter. They are subsequently monitored using UV spectrophotometry at 296 nm. Amount of drug that was captured is indicated by the difference between the amount of drug that was originally used and the amount of drug that is in the wash (equation-1).[30]

$$\% \text{ Drug entrapment} = \frac{A1}{A2} \times 100 --(1)$$

where, A2 – Amount of drug in washings, A1 – Amount of drug initially loaded.

Swelling Index

Using chitosan hydrogels in an HCL buffer with a pH of 1.2 for 8 hours allowed us to study the hydrogel's swelling property as it relates to pH. The hydrogels were taken out of the water solution at regular intervals, and any surplus water was drained out using filter paper. Then, the contents were weighed, and the process was repeated until equilibrium was reached. Following equation (Equation-2) was used at various times to calculate degree of swelling (%):

$$\% \text{ Swelling} = \frac{\text{Initial wt} - \text{Final wt.}}{\text{Initial wt.}} \times 100 --(2)$$

Evaluation of Mucoadhesion

The *in vitro* washout approach was used to assess the mucoadhesive characteristics of the composite hydrogel that was created, as previously mentioned.[31] This was accomplished by removing mucosa from rats' stomachs and then tying it to a glass slide using thread. After preparing tissue sample, which included rinsing it, approximately 25 bigger hydrogel particles were distributed over it. The slide was then suspended in one of grooves of USP pill disintegrator, and a gradual, regular up and down motion of the tissue was started. Heat liquid to 37±1 ℃ for testing. We stopped machine and counted amount of fragments attached to tissue at each 1-hour interval. Here is equation (Eq.-3) that gives proportion of mucoadhesion:

$$\% \text{ mucoadhesion} = \frac{P1}{P2} \times 100 --(3)$$

where,

P2- initial no. of hydrogel pieces

P1- no. of adhered hydrogel pieces

***In vitro* release**

An experiment was conducted in which a 100 mg polymer drug composite hydrogel was immersed in 100 mL of phosphate buffer (pH 2, biomimetic pH), while temperature was kept at 37±1 °C and the buffer was swirled magnetically at 100 rpm. Over course of 24 hours, we took 1 mL samples from combination at different intervals. To keep the sink condition constant, new buffer was added to volume after sampling. At 296 nm, a UV-vis spectrophotometer (Shimadzu Mini-1240, Japan) was used to ascertain telmisartan content in sample.[32,33]

Analysis of release data

We utilised the release data gathered by the aforementioned technique to develop the release mechanism according to the Ritger and Peppas model[34, 35]. Equation (4) was used to estimate the diffusion exponent "n" using the initial 60% cumulative release data:

$$\frac{M_t}{M_1} = Kt^n --(eq-4)$$

Drug release at time t is denoted as Mt, the total amount of drug released at kinetic constant K is M1, and diffusion exponent n describes release mechanism. Fickian release is indicated by a 'n' value of 0.43 or less, while non-Fickian release, including diffusion controlled and swelling controlled drug release, is denoted by a 'n' value between 0.43 and 0.85. Case II transport, characterised by polymer chain elongation and entanglement, is indicated by a 'n' value of 0.85 or above.

Statistical analysis

All data were stated as mean ± S.D. of triplicate results obtained from easy studies, and the same were investigated by BioStat version 2009 software for Windows.

Results and discussions

Optimization of hydrogel formulations using CCD

The LBG:TC IPN hydrogel utilised in this work was prepared by Stat-Ease Design Expert version 13, which is a response surface methodology program. Investigating the effects of mucoadhesive efficiency (Y1), particle size (Y2), and drug release Q24h (Y3) of IPN hydrogel containing telmisartan are the primary formulation factors for experimental design. A central composite design is used. Impact of carob gum, thiolated chitosan, and TPP concentrations on the aforementioned processes in IPN hydrogels was the subject of an experimental investigation. A total of seventeen formulations were prepared in accordance with a central composite design (CCD) in three variables, three responses, and three midpoints (Table 2).

Optimization study

Under ideal test conditions, the particle size (µm), MA (%), and release (%) of the produced hydrogel particles entrapping telmisartan were impacted by the concentrations

Table 3: Response model and statistical parameters achieved from ANOVA for CCD

Responses	Adjusted R^2	Predicted R^2	Model P value	Adequate precision	%CV
Particle size	0.9235	0.9089	<0.0002	12.18	10.88
Entrapment efficiency	0.9832	0.9577	<0.0005	15.20	8.21
Drug release	0.9509	0.9035	<0.0001	10.89	9.57

Table 4: Polynomial model equations

Polynomial model	
Mucoadhesive (Y1)	-2.59774-105.60599 TC -33.27142 LBG+44.68340 TPP +79.00000 TC*LBG+10.00000 TC*TPP-3.40000 LBG*TPP-4.69223 TC^2-18.14362 LBG^2-4.60004 TPP^2
Particle size (Y2)	-362.37905+413.70859 TC+81.92181 LBG+98.02797 TPP-9.00000 TC * LBG-54.00000 TC * TPP+1.40000 LBG * TPP-37.80571 TC^2-60.36312 LBG^2-2.19105 TPP^2
Drug release (Y3)	-503.26301+437.00256 TC +73.54978 LBG+110.61524 TPP +81.81290 TC * LBG-17.87644 TC * TPP-17.85058 LBG * TPP-178.63101 TC^2 -27.52349 LBG^2-6.55301 TPP^2

Table 5: Value of responses under optimal assay conditions

Point Prediction	Particle size (μm)	Mucoadhesive (%)	Drug release (%)
Predicted	179.03	75.00	99.86
Observed	181.05±1.04	77.2±1.38	97.99±3.22
% error	1.12	2.93	-1.87

Table 6. % of particles adhering to tissue in Phosphate buffer pH 7.4

Formulations	Time in hours					
	1 hr	2hr	4 hr	6 hr	8 hr	10 hr
LBG:TC hydrogel	81±3.2	78±2.8	73±3.9	70±2.2	65±4.6	32±2.5

of LBG, TC, and TPP. The parameters were optimised using the following polynomial equation.

$Y = \alpha_0 + \alpha_1X_1 + \alpha_2X_2 + \alpha_3X_3 + \alpha_4X_1X_2 + \alpha_5X_2X_3 + \alpha_6X_1X_3 + \alpha_7X_1^2 + \alpha_8X_2^2 + \alpha_9X_3^2$

Response surface methodology

Effect of process variable on mucoadhesive properties

Perturbation plot further clarified relationship among independent and dependent variables by revealing primary effects of A, B, and C on mucoadhesive (Y_1) of LBG: TC hydrogel. Figure 1 a, Figure 1 b, Figure 1 c, Figure 1 d demonstrates that A is most influential variable on Y_1, followed by C, which has a moderate effect, and finally B, which has a little effect.

Effect of process variable on particle size

The primary effects of A, B, and C on particle size (Y2) of LBG: TC hydrogel were shown in the perturbation plot, which further clarified link between dependent and independent variables. Hierarchy of effects shown in Figure 2 a, Figure 2b, Figure 2c, Figure 2d is as follows: B has most significant impact on Y2, C has a moderate influence, and A has a negligible one.

Effect of process variable on drug release

More complex was effect of factors on medication release. In order to optimise the independent variables, the 12-hour drug release schedule (Q12h) was selected. The drug release research mimicked the circumstances found in the intestines. The table provides the mathematical relationship for measured response, drug release Y3, in form of a polynomial equation.

A perturbation plot illustrating the primary impacts of A, B, and C on drug release (Y3) of LBG: TC hydrogel further clarified link between dependent and independent variables. Based on data presented in Figure 3 a, Figure 3b, Figure 3c, Figure 3d, it is evident that C has most impact on Y3, followed by A with a moderate effect, and finally B with a small impact.

ANOVA

A number of statistical characteristics, including adjusted R^2, predicted R^2, model P values, sufficient precision, and %CV, are displayed in Table 3. Table 3 demonstrates that the expected R^2 and adjusted R_2 for Y_1, Y_2, and Y_3 are highly congruent.

Polynomial model equations

The responses of Y1, Y2 and Y3 are equated and shown in Table 4.

Point prediction

The formulation and measurement of responses involved LBG:TC IPN hydrogel particles. Values of the anticipated and observed design responses were compared. The percentage of errors was computed in order to validate the procedure. Y1, Y2, and Y3 were all found to be in agreement with the projected value. The effectiveness of the optimisation process was demonstrated by this.

Particle size, MA, and drug release can all be optimised in LBG:TC IPN hydrogels. This method was used to discover a set of parts. Predictions for the particle size, MA, and drug release of LBG:TC IPN hydrogel particles with a composition of 1.5% LBG, 1.47% TC, and 5.52% TPP were 179.03 nm, 75.00%, and 99.96%, respectively.

The LBG: TC IPN hydrogel particles were determined to have a suitability of 0.917, which falls within the range of 0.8 to 1, indicating that the formulation quality was satisfactory and outstanding. Assuming the number was less than 0.63, the formulation was deemed to have poor quality **(Figure 4)**.

Predicted and observed values

Table 5 displays obtained experimental and anticipated values with their respective percentage errors.

% error = (observed value-predicted value)/predicted value x 100

optimized hydrogel particles containing telmisartan showed MA of 77.2 ± 1.38%, size of 181.05 ± 1.04 and Q12h (%) of 97.99 ± 3.22% with small error values (1.12, 2.93 and -1.87 respectively). That the mathematical models derived from the CCD design fit the data well is evident from this. That the optimised technique was able to reliably forecast operating parameters for hydrogel production for a mucoadhesive drug delivery system was further established. Additional characterisation of the chosen formulation was then performed.

FTIR

Figure 5 shows the FTIR spectrum of the pure drug. Vibrational band at 3450 cm^{-1} is attributed to O-H stretching of -COOH bond. Near 2900 cm^{-1}, aromatic C-H stretching vibrations are visible, which is due to -OH bending. At 1385 cm^{-1}, C=C ring vibrations of aromatic ring are visible. C-N stretching of imidazole ring of drug is near 1350-1200 cm^{-1}. There were noticeable peaks at 3750 and 3000 cm^{-1} in FTIR spectrum of both pure and cysteine functionalised (Thiolated) chitosan. These peaks were caused by stretching vibrations of hydroxyl group, which overlapped with N-H stretching of glucosamine moiety of the chitosan. Additionally, there was a vibrational band near 2850 cm^{-1}, which was detected as CH bond of CH_2 of the TPP moiety. Another band associated with methylene bending was seen[36] at 1375 cm^{-1}. The stretching vibration of the O-H groups was attributed to a broad vibrational band that emerged at around 3367.71 cm^{-1} in the case of locust bean gum. C-O stretching is responsible for the vibrational bands at 1030 cm^{-1}, whereas C-H stretching is responsible for the bands at 2885 cm^{-1}. The CH_2 scissoring vibration is allocated[37] a band near 1385 cm^{-1}. The main drug peaks in the fingerprint region were easily discernible in the case of the IPN hydrogel formulation. There observed a noticeable lack of aromatic -CH stretching vibrations near 2900 cm^{-1} compared to the pristine drug molecule. However, between 2750 and 3600 cm^{-1}, a wide band was discernible as a result of the -OH vibration of the water molecule, as well as the -OH and -NH stretching of telmisartan. On top of that, the aromatic ring vibration transmittance percentage drops between 1600 and 1800 cm^{-1}.

SEM

Tiny needle-shaped crystals are visible in pure medicines. In contrast, the hydrogel formulation appeared as a soft powder under low magnification, featuring rough morphological surfaces and structural porosity. The drug crystals (X5000) were placed onto the polymer at a greater magnification. The powdered hydrogel's surface pores are believed to enhance medication solubility and bioavailability by facilitating the imbibition of solvents and biological fluids (Figure 6).

Mucoadhesive studies

Table 6 displays the results of the mucoadhesion test that was conducted on LBG: TC hydrogel particles. The test was carried out continuously for 10 hours at a pH of 7.4. At a pH of 7.4, 61% of the hydrogel particles remained attached to the tissue after 10 hours. As the amount of polymer increased, LBG and thiolated chitosan demonstrated better mucoadhesion. The reason behind this is that chitosan has a high concentration of thiolate anions, which promote mucoadhesion through covalent attachment, because of the reaction with thiol groups in the mucus gel layer.

***In-vitro* Drug Release**

Figure 7 to Figure 11 shows the telmisartan *in vitro* drug release profile from the LBG:TC hydrogel. In a phosphate buffer pH 7.4, the release of TEL from LBG:TC hydrogel demonstrated a prolonged release of the drug. The presence of hydrophilic thiolated groups in thiolated chitosan causes it to connect to amino groups via hydrogen bonds, which disrupts intermolecular hydrogen bonds and results in increased space for water in the polymer matrix. This causes the progressive release of the compound. The thiolated chitosan polymer swelled many times its original size. An electrostatic repulsive force between the negative charges is generated when the concentration of the thiolated anion increases, as shown by the results. Another possible explanation for the hydrophobic medication's sluggish release from the LBG:TC hydrogel is the formulation complex that exists between the drug and the thio group on the polymer chain. Complex formulations incorporate a number of variables, including drug-thiolated chitosan hydrogen bonding and Wanderwall interactions. Pharmacological release rates are inversely proportional to particle polymer concentration, as demonstrated by the *in vitro* release of TEL from the hydrogel. This may be because the thiopolymer has a greater capacity to swell, which in turn increases the gelation rate (the length of the diffusion path) for the medication and so slows its release from the formulation. Suppressing burst drug release in the stomach and regulating drug release profiles in the variable pH environment of the gastrointestinal tract were made possible by the presence of each LBG polymer component in the hydrogel. This was necessary because TC particles alone could not withstand the shock effect at acidic pH. The novel hydrogel method showed promise for regulated medication delivery. As a result of these transformations, the polymers go from a glassy to a rubbery state, and the polymer chains relax and absorb water.[38] Swelling causes the volume to expand significantly, which moves the diffusion limits and makes solving Fick's second equation of diffusion more difficult. In order to further process the release data, the equation provided by Ritger and Peppas was used. Fickian diffusion and case II transport, which describe the release of drugs from a swelling polymer, are two seemingly separate mechanisms of drug transport that are superimposed in this equation.[39] Drug release regulated by swelling occurs when "n" is set to 1.0 while diffusion-controlled release occurs when "n" is set to 0.5. Both phenomena (anomalous transport) can be indicated by n values between 0.5 and 1.0. Anomaly transport was shown by the optimised formulation's regression coefficient n value of 0.9734. The drug release from LBG:TC hydrogel containing telmisartan was shown to be both swelling-controlled and diffusion-controlled by the anomalous diffusion mechanism.[40]

CONCLUSION

From point of view of drug delivery, hydrogels based on LBG:TC can be used to localize drugs, increase concentration of the drug at site of action and subsequently reduce unwanted side effects of telmisartan. LBG:TC hydrogel formulation was optimized using CCD model and characterized. Experimental findings were obtained for different combinations of independent variables, including LBG, TC, and TPP, and they were found to be consistent with the design model. The variables studied included quantitative particle size, mucoadhesiveness, and *in vitro* drug release responses. A hydrogel loaded with telmisartan was formulated using an ionic gelation technique and evaluated for mucoadhesive strength and drug release under simulated physiological conditions. The formulation showed good mucoadhesive properties and prolonged drug release. Drug release from hydrogel was monitored by a non-fictitious mechanism. Based on this, we conclude that the new hydrogel is one of the best options for improving the bioavailability of telmisartan.

Acknowledgements

The Authors are thankful to the unknown reviewers of the journal for their valuable time in peer review of the manuscript.

REFERENCES

1. Patra CN, Dutta P, Sruti J, Rao MB. Floating microspheres: recent trends in the development of gastroretentive floating drug delivery system. International Journal of Pharmaceutical Sciences and Nanotechnology (IJPSN). 2011; 31; 4(1):1296-1306. https://doi.org/10.37285/ijpsn.2011.4.1.2
2. Garg R, Gupta GD. Gastroretentive floating microspheres of silymarin: preparation and *in vitro* evaluation. Tropical journal of pharmaceutical research. 2010; 9(1): 59-66. DOI:10.4314/tjpr.v9i1.52037
3. Mukund JY, Kantilal BR, Sudhakar RN. Floating microspheres: a review. Brazilian Journal of Pharmaceutical Sciences. 2012; 48:17-30.
4. Ries UJ, Mihm G, Narr B, Hasselbach KM, Wittneben H, Entzeroth M, Van Meel JC, Wienen W, Hauel NH. 6-Substituted benzimidazoles as new nonpeptide angiotensin II receptor antagonists: synthesis, biological activity, and structure-activity relationships. Journal of medicinal chemistry. 1993; 36(25):4040-4051.
5. Cagigal E, Gonzalez L, Alonso RM, Jimenez RM. pKa determination of angiotensin II receptor antagonists (ARA II) by spectrofluorimetry. Journal of pharmaceutical and biomedical analysis. 2001; 1; 26(3):477-486. doi: 10.1016/s0731-7085(01)00413-7.
6. Stangier J, Su CA, Roth W. Pharmacokinetics of orally and intravenously administered telmisartan in healthy young and elderly volunteers and in hypertensive patients. Journal of International Medical Research. 2000; 28(4):149-167.
7. Sekar V, Chellan VR. Immediate release tablets of telmisartan using superdisintegrant-formulation, evaluation and stability studies. Chemical and Pharmaceutical Bulletin. 2008; 1; 56(4):575-577. doi: 10.1248/cpb.56.575.
8. Zhang Y, Jiang T, Zhang Q, Wang S. Inclusion of telmisartan in mesocellular foam nanoparticles: drug loading and release property. European journal of pharmaceutics and biopharmaceutics. 2010; 1; 76(1):17-23.
9. Zhang Y, Zhi Z, Jiang T, Zhang J, Wang Z, Wang S. Spherical mesoporous silica nanoparticles for loading and release of the poorly water-soluble drug telmisartan. Journal of Controlled Release. 2010;3; 145(3):257-263. doi: 10.1016/j.jconrel.2010.04.029.
10. Patel J, Kevin G, Patel A, Raval M, Sheth N. Design and development of a self-nanoemulsifying drug delivery system for telmisartan for oral drug delivery. International journal of pharmaceutical investigation. 2011;1(2):112.
11. Singh M, Murugan NA, Kongsted J, Zhan P, Banerjee UC, Poongavanam V. Molecular Insights from Spectral and Computational Studies on Crystalline and Amorphous Telmisartan. Crystal Growth & Design. 2024; 25; 24(15):6354-6363.
12. Zhong L, Zhu X, Yu B, Su W. Influence of alkalizers on dissolution properties of telmisartan in solid dispersions prepared by cogrinding. Drug development and industrial pharmacy. 2014; 1; 40(12):1660-1669. doi: 10.3109/03639045.2013.841188.
13. Zhong L, Zhu X, Luo X, Su W. Dissolution properties and physical characterization of telmisartan–chitosan solid dispersions prepared by mechanochemical activation. AAPS PharmSciTech. 2013;14:541-550.
14. Tran PH, Tran HT, Lee BJ. Modulation of microenvironmental pH and crystallinity of ionizable telmisartan using alkalizers in solid dispersions for controlled release. Journal of Controlled Release. 2008;2;129(1):59-65.
15. Kaur P, Ghildiyal S, Soni S. Development and Evaluation of Hydrodynamically Balanced System of Tramadol Hydrochloride by Using Chitosan and Locust Bean Gum. Journal of Internal Medicine and Emergency Research 2020; 1:1-20. https://doi.org/10.37191/Mapsci-2582-7367-1(2)-012. https://doi.org/10.37191/Mapsci-2582-7367-1(2)-012
16. Talaat HA, Sorour MH, Aboulnour AG, Shaalan HF, Ahmed EM, Awad AM, Ahmed MA. Development of a multi-component fertilizing hydrogel with relevant techno-economic indicators. American-Eurasian Journal of Agricultural & Environmental Sciences. 2008. 19;3(5):764-770.
17. Jia X, Kiick KL. Hybrid multicomponent hydrogels for tissue engineering. Macromolecular bioscience. 2009;11;9(2):140-156.
18. Fujioka-Kobayashi M, Ota MS, Shimoda A, Nakahama KI, Akiyoshi K, Miyamoto Y, Iseki S. Cholesteryl group-and acryloyl group-bearing pullulan nanogel to deliver BMP2 and FGF18 for bone tissue engineering. Biomaterials. 2012;1;33(30):7613-7620. doi: 10.1016/j.biomaterials.2012.06.075.

19. Shimoda A, Chen Y, Akiyoshi K. Nanogel containing electrospun nanofibers as a platform for stable loading of proteins. RSC Advances. 2016; 6(47):40811-40817.
20. Shimoda A, Sawada SI, Akiyoshi K. Intracellular protein delivery using self-assembled amphiphilic polysaccharide nanogels. Intracellular delivery II: fundamentals and applications. 2014:265-274.
21. Pardeshi CV, Belgamwar VS. Controlled synthesis of N, N, N-trimethyl chitosan for modulated bioadhesion and nasal membrane permeability. International journal of biological macromolecules. 2016;1;82:933-944.
22. Ren J, Li Q, Dong F, Feng Y, Guo Z. Phenolic antioxidants-functionalized quaternized chitosan: Synthesis and antioxidant properties. International journal of biological macromolecules. 2013;1;53:77-81. doi: 10.1016/j.ijbiomac.2012.11.011.
23. Kurita K, Ikeda H, Shimojoh M, Yang J. N-phthaloylated chitosan as an essential precursor for controlled chemical modifications of chitosan: Synthesis and evaluation. Polymer Journal. 2007;39(9):945-952.
24. Baba Y, Noma H, Nakayama R, Matsushita Y. Preparation of chitosan derivatives containing methylthiocarbamoyl and phenylthiocarbamoyl groups and their selective adsorption of copper (II) over iron (III). Analytical sciences. 2002; 18(3):359-361.
25. Furusaki E, Ueno Y, Sakairi N, Nishi N, Tokura S. Facile preparation and inclusion ability of a chitosan derivative bearing carboxymethyl-β-cyclodextrin. Carbohydrate Polymers. 1996; 1; 29(1):29-34.
26. Stefanov I, Hinojosa-Caballero D, Maspoch S, Hoyo J, Tzanov T. Enzymatic synthesis of a thiolated chitosan-based wound dressing crosslinked with chicoric acid. Journal of materials chemistry B. 2018; 6(47):7943-7953. doi: 10.1039/c8tb02483a.
27. Esquivel R, Juárez J, Almada M, Ibarra J, Valdez MA. Synthesis and characterization of new thiolated chitosan nanoparticles obtained by ionic gelation method. International Journal of Polymer Science. 2015;(1):502058.
28. Meena LK, Raval P, Kedaria D, Vasita R. Study of locust bean gum reinforced cyst-chitosan and oxidized dextran based semi-IPN cryogen dressing for hemostatic application. Bioactive Materials. 2018;1;3(3):370-384.
29. Inamdar NN, Mourya V. Thiolated chitosan preparation, properties, and applications. Chitin and Chitosan Derivatives: Advances in Drug Discovery and Developments; CRC Press/Taylor and Francis: Boca Raton, FL, USA. 2013:121-150. DOI:10.1201/b15636-8
30. Ganesh M, Ubaidulla U, Rathnam G, Jang HT. Chitosan-telmisartan polymeric cocrystals for improving oral absorption: *In vitro* and in vivo evaluation. International journal of biological macromolecules. 2019;15;131:879-885.
31. Mane VB, Killedar SG, More HN, Tare HL, Evaluation of acute oral toxicity of the Emblica officinalis Phytosome Formulation in Wistar Rats. International Journal of Drug Delivery Technology. 2022; 12(4):1566-1570.
32. Kataria K, Gupta A, Rath G, Mathur RB, Dhakate SR. In vivo wound healing performance of drug loaded electrospun composite nanofibers transdermal patch. International journal of pharmaceutics. 2014 ;20;469(1):102-110. DOI:10.1016/j.ijpharm.2014.04.047
33. Higuchi T. Rate of release of medicaments from ointment bases containing drugs in suspension. Journal of pharmaceutical sciences. 1961;1; 50(10):874-875.
34. Ritger PL, Peppas NA. A simple equation for description of solute release II. Fickian and anomalous release from swellable devices. Journal of controlled release. 1987;1;5(1):37-42.
35. Yasam VR, Jakki SL, Natarajan J, Kuppusamy G. A review on novel vesicular drug delivery: proniosomes. Drug delivery. 2014;1; 21(4):243-249.
36. Mane V, Killedar S, More H, Salunkhe S, Tare H. Development and Validation of a Novel Bioanalytical Method for Estimating Epigallocatechin 3 Gallate in Wistar Rat Plasma by RP-HPLC Employing Gradient Elution Techniques. Journal of Research in Pharmacy. 2023; 1;27(3). DOI: https://doi.org/10.52756/ijerr.2023.v36.004
37. Ganesh M, Jeon UJ, Ubaidulla U, Hemalatha P, Saravanakumar A, Peng MM, Jang HT. Chitosan cocrystals embedded alginate beads for enhancing the solubility and bioavailability of aceclofenac. International journal of biological macromolecules. 2015;1;74:310-317.
38. Mane V, Killedar S, More H, Tare H. Preclinical study on camellia sinensis extract-loaded nanophytosomes for enhancement of memory-boosting activity: optimization by central composite design. Future Journal of Pharmaceutical Sciences. 2024;1;10(1):66. DOI:10.1186/s43094-024-00639-9
39. Mane V, Killedar S, More H, Nadaf S, Salunkhe S, Tare H. Novel Phytosomal Formulation of Emblica officinalis Extracts with Its In Vivo Nootropic Potential in Rats: Optimization and Development by Box-Behnken Design. Journal of Chemistry. 2024 ;(1):6644815.
40. Mane VA, Killedar SU, More HA, Gaikwad AS, Tare HA. A novel RP-HPLC gradient elution technique for bioanalytical method development and validation for estimating gallic acid in wistar rat plasma. International Journal of Applied Pharmaceutics. 2023;7;15(2):153-160. DOI:10.22159/ijap.2023v15i2.47278